Journal of Sound and Vibration (1997) **206**(1), 23–38

ANALYSIS OF VIBRATING CIRCULAR PLATES HAVING NON-UNIFORM CONSTRAINTS USING THE MODAL PROPERTIES OF FREE-EDGE PLATES: APPLICATION TO BOLTED PLATES

M. Amabili† and R. Pierandrei

Dipartimento di Meccanica

and

G. Frosali

Dipartimento di Matematica "V. Volterra", Università di Ancona, I-60131 Ancona, Italy

(*Received* 3 *January* 1996, *and in final form* 8 *April* 1997)

The free vibrations of a circular plate having elastic constraints variable according to the angular co-ordinate are investigated. The non-uniform translational and rotational stiffness of the constraints are expanded in a Fourier series; it is assumed that the system presents a symmetry axis. The mode shapes are expanded in a Fourier–Bessel series by using the Rayleigh–Ritz method. The eigenfunctions of the free-edge circular plate vibrating in vacuum are assumed as admissible functions. This choice allows one to compute the potential energy of the plate using the kinetic energy of single modes of free-edge plates. The effect of the in-plane load is included and internal constraints are studied. By using the same technique, the free vibrations of a circular plate resting on an annular, non-uniform, Winkler foundation are investigated. Numerical results are given for the cases studied already, in order to validate the proposed method, and for bolted (or riveted) plates fixed by different numbers of bolts.

1. INTRODUCTION

Since plates are common components of structures, plants and containers in various industrial fields, knowledge of their modal behaviour is very useful for design engineers and researchers. Many papers deal with the free vibrations of circular plates. The first studies on this topic are attributed to Poisson [1] and Kirchhoff [2]. Leissa [3] has presented a thorough summary of the previously published literature up to the year 1965. In references [4–7] the free vibrations of free-edge circular plates were studied and both the frequency and mode shape parameters are given for different values of Poisson's ratio ν. In particular, Itao and Crandall [6] have published the lowest 701 eigenvalues and corresponding eigenvectors for $\nu = 0{\cdot}33$ and Amabili *et al*. [7] have studied the influence of the Poisson's ratio in the full range from 0 to 0·5 of the possible values. Numerical results relative to simply supported edge have been given by Leissa and Narita [8] for the full range of the possible Poisson's ratios and by Leissa [3] for clamped plates. A complete work on the free vibration of circular plates having axisymmetric edge constraints is that of Azimi [9], where the receptance method was used.

† Present address: Dipartimento di Ingegneria Industriale, Università di Parma, 43100 Parma, Italy.

0022–460X/97/360023 + 16 $25.00/0/sv971054

The practical realization of a simply supported or clamped plate to be used in an experimental test is sometimes a problem. In fact, the realization of an infinite stiff constraint for flexural edge displacement and rotation is obviously impossible and only an approximation of the ideal constraint is possible. A study of the finite stiffness of uniform constraints for rectangular plates has been given in reference [10]. Actually, the plate boundary conditions are often realized by using bolts or rivets, so that the boundary conditions are not uniform. Therefore, the real constraint is an elastic edge support, whose stiffness is not constant, due to bolts, and this is a function of the co-ordinate describing the edge. A study of circular plates having non-uniform edge constraints has been reported [11], in which numerical results were given for the case where the rotational stiffness varies as one cosinusoidal wave; in this paper the Fourier expansion of the variable edge constraints was introduced. Also Narita and Leissa [12, 13] studied elastic translational and rotational constraints that are not uniform around the edge of circular plates; they obtained a series solution by imposing the boundary conditions and give many numerical results. Moreover, the free vibrations of a circular plate clamped on part of its boundary and simply supported on the remainder have been previously studied [14, 15]; in particular Bartlett [14] used an interesting variational approach. Hirano and Okazaki [16] studied a circular plate clamped, simply supported or free on part of its boundary and simply supported, free or clamped, respectively, on the remainder.

In the present paper, the free vibrations of a circular plate with flexible constraints having variable stiffness according to the angular co-ordinate are investigated. Both the flexible constraints to displacement and rotation are considered; these constraints can also be internal with respect to the plate edge. The non-uniform translational and rotational stiffness of the constraints is expanded into a Fourier series; only cosines are considered, due to the assumed presence of a symmetry axis, as in any equidistant bolt disposition. Due to the assumed symmetry of the problem, two families of modes, symmetric and antisymmetric ones, are obtained. The plate is assumed to be thin and made of linear elastic, homogeneous and isotropic material, so that the classic theory of plates is applicable. The effect of an uniform in-plane load is included. The mode shapes are expanded in a Fourier–Bessel series by using the Rayleigh–Ritz method [17, 18]. As admissible functions, the eigenfunctions of the free-edge circular plate vibrating in a vacuum are assumed. This choice allows one to compute the potential energy of the plate by using the kinetic energy of modes of free-edge plates. As a consequence of the inclusion principle, the computed eigenvalues approach the actual eigenvalues asymptotically and from above, as the number of terms considered in the series increases; also the corresponding eigenvectors approach the actual mode shapes. The method used in the present paper to obtain the solution is therefore different from that used in references [11–13] and is based on the artificial spring method [19, 20]. The advantage is that it can also be used to study circular plates joined to quite complex structures; in fact the artificial spring method has been introduced in substructuring. Moreover many complicating effects, e.g. in-plane load, foundations and added distributed or lumped masses, can be included in the study with little complication of the theory.

The aim of this paper is to apply the method to analyze the constraint given by bolts or rivets; in fact it seems that a similar method has been applied to bolted (or riveted) plates only in a recent paper of the present authors [21]. Circular plates are mechanical components used to close circular pressure vessels, circular tanks and pipes, and are usually connected to other structural elements by using bolts or rivets. This constraint gives restriction to translation and rotation of the plate at the bolts; therefore one has a constraint that is not uniform around the mean radius where the bolts are placed. Moreover bolts generate a compressive in-plane stress inside the plate, due to the Poisson

effect [22]. In fact, a bolt gives a compressive pressure to the plate. When applying this pressure, because of the Poisson effect, a portion of the plate expands in an inward direction. A similar expansion is given by other bolts. Due to the combined "inwards" effects an in-plane stress is generated inside the plate. This compressive in-plane stress gives a reduction in the natural frequencies of the plate [22–25]. This reduction can be significant for very thin plates.

Numerical results are obtained for bolted plates fixed by a different number of bolts. The proposed technique is then used to study the free vibrations of a circular plate rested on an annular Winkler foundation having stiffness variable according to the angular co-ordinate.

2. METHOD OF SOLUTION

A polar co-ordinate system (O, r, θ) is introduced, with the origin at the centre of a circular plate of radius a and uniform thickness h. By using the Rayleigh–Ritz method, the flexural mode shapes W of the plate are expanded in a Fourier–Bessel series at both the radial and angular co-ordinates. In particular, the trial functions in the radial direction are the mode shapes of free-edge plates vibrating in vacuum, also including the two rigid body modes (uniform displacement and rotation around a diameter) of the free-edge plate. This choice gives a complete set of orthogonal trial functions and allows one to simplify the computation of the potential energy of the system. The trial functions in the angular direction are given by the classic Fourier series. The flexural mode shapes W with the Fourier coefficients a_{mn} and b_{mn}, and the admissible radial functions W_{mn}, are described by

$$W(r,\theta) = \sqrt{2}a_{00} + \sum_{n=1}^{\infty} W_{0n}(r)a_{0n} + 2\frac{r}{a}(a_{10}\cos\theta + b_{10}\sin\theta)$$

$$+ \sum_{n=1}^{\infty} \mathrm{W}_{1n}(r)(a_{1n}\cos\theta + b_{1n}\sin\theta) + \sum_{m=2}^{\infty}\sum_{n=0}^{\infty} W_{mn}(r)[a_{mn}\cos(m\theta)$$

$$+ b_{mn}\sin(m\theta)], \tag{1}$$

where

$$W_{mn}(r) = A_{mn}\mathrm{J}_m(\lambda_{mn}r/a) + C_{mn}\mathrm{I}_m(\lambda_{mn}r/a), \tag{2}$$

m and n are the numbers of nodal diameters and circles in the mode shape of a free-edge plate, J_m and I_m the Bessel and the modified Bessel functions of the first kind, A_{mn} and C_{mn} are the mode shape constants and λ_{mn} is the frequency parameter. In equation (1) it has been assumed that the eigenfunctions of the free-edge plate are the admissible functions, so that the values of A_{mn}, C_{mn} and λ_{mn} must be given for a free-edge plate. These are tabulated in reference [6] for Poisson's ratio $\nu = 0{\cdot}33$ and in reference [7] for other ν values. The frequency parameter λ_{mn} is related to the circular frequency by $\omega_{mn} = (\lambda_{mn}/a)^2\sqrt{(D/(\rho_P h))}$, where D is the flexural rigidity of the plate, $D = (Eh^3)/(12(1-\nu^2))$, E is the Young's modulus and ρ_P is the mass density of the plate material. To simplify the computations, the mode shape constants are normalized according to

$$\int_0^1 W_{mn}^2(a\rho)\rho\,\mathrm{d}\rho = 1, \tag{3}$$

where $\rho = r/a$; the constants of the rigid body modes have already been normalized in equation (1).

The reference kinetic energy of the plate is defined by

$$T_P^* = \frac{1}{2}\rho_P h \int_0^{2\pi}\int_0^a W^2(r) r \, \mathrm{d}r \, \mathrm{d}\theta. \tag{4}$$

By using the orthogonality of the assumed trial functions, the following expression for T_P^* is obtained:

$$T_P^* = \frac{1}{2}\rho_P h a^2 \left[2\pi \sum_{n=0}^{\infty} a_{0n}^2 + \pi \sum_{m=1}^{\infty}\sum_{n=0}^{\infty} (a_{mn}^2 + b_{mn}^2) \right]. \tag{5}$$

As a consequence of the trial functions being the actual mode shapes of free-edge plates, the maximum potential energy of the plate can be expressed by using the well-known modal properties of the free-edge plates. More precisely, each term of the right side of equation (1) has the same shape as the eigenvector of free-edge plates with the same number of circular and diametral nodes. Thus, the maximum potential energy associated with each term of $W(r, \theta)$ can be expressed as the product of the reference kinetic energy of the corresponding mode of the free-edge plate for the squared circular frequency ω_{mn}^2 of the mode itself. Therefore, the maximum potential energy stored by the plate can be written as the sum

$$V_P = \frac{1}{2}\rho_P h a^2 \left[2\pi \sum_{n=0}^{\infty} a_{0n}^2 \omega_{0n}^2 + \pi \sum_{m=1}^{\infty}\sum_{n=0}^{\infty} (a_{mn}^2 + b_{mn}^2)\omega_{mn}^2 \right]. \tag{6}$$

By using the relation between the circular frequency ω_{mn} and the frequency parameter λ_{mn}, equation (6) can be transformed into

$$V_P = \frac{1}{2}\frac{D}{a^2} \left[2\pi \sum_{n=0}^{\infty} a_{0n}^2 \lambda_{0n}^4 + \pi \sum_{m=1}^{\infty}\sum_{n=0}^{\infty} (a_{mn}^2 + b_{mn}^2)\lambda_{mn}^4 \right], \tag{7}$$

The maximum potential energy of the elastic distributed springs which simulate the flexible translational constraint at the distance $R \leqslant a$ from the plate centre is given by

$$V_T = \frac{1}{2}\int_0^{2\pi} l(\theta) W^2(R, \theta) R \, \mathrm{d}\theta. \tag{8}$$

It is assumed that the flexible constraints have a symmetry axis, as for any equidistant bolt disposition; the stiffness $l\,(\mathrm{N\ m^{-2}})$ of the distributed springs simulating the

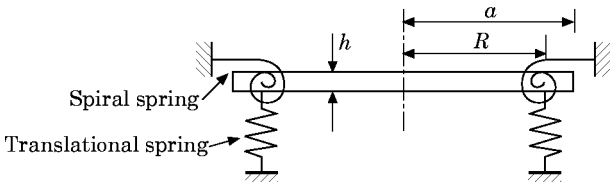

Figure 1. Circular plate having elastic constraints.

translational edge constraint (see Figure 1) can be expanded into the Fourier cosine series

$$l(\theta) = \sum_{k=0}^{\infty} l_k \cos(k\theta). \tag{9}$$

Due to the symmetry of the plate and boundary conditions, two different sets of modes are found: symmetric and antisymmetric ones. First of all, the symmetric modes are studied; in this case, all the coefficients b_{mn} are zero. Therefore equation (1) can be written in the form

$$W(r, \theta) = \sum_{m=0}^{\infty} \sum_{n=0}^{\infty} W_{mn}(r) a_{mn} \cos(m\theta), \tag{10}$$

where the definition of W_{mn}, equation (2), is extended to include $W_{00} = \sqrt{2}$ and $W_{10} = 2r/a$. By substituting equation (2) in equation (10) and then equations (9) and (10) in equation (8), it is found

$$V_T = \frac{1}{2} \int_0^{2\pi} \left[\sum_{k=0}^{\infty} l_k \cos(k\theta) \right] \left[\sum_{m=0}^{\infty} \sum_{n=0}^{\infty} W_{mn}(R) a_{mn} \cos(m\theta) \right]^2 R \, \mathrm{d}\theta. \tag{11}$$

The result of the quadrature of equation (11) is

$$V_T = \tfrac{1}{2} R \sum_{m=0}^{\infty} \sum_{s=0}^{\infty} \sum_{n=0}^{\infty} \sum_{i=0}^{\infty} \sum_{k=0}^{\infty} \psi_{msk} l_k a_{mn} a_{si} W_{mn}(R) W_{si}(R), \tag{12}$$

where

$$\psi_{msk} = \int_0^{2\pi} \cos(m\theta) \cos(s\theta) \cos(k\theta) \, \mathrm{d}\theta = \left\{ \begin{array}{ll} 2\pi, & \text{if } m = s = k = 0 \\ \pi, & \text{if } k = 0 \text{ and } m = s \neq 0 \\ \pi, & \text{if } m = 0 \text{ and } s = k \neq 0 \\ \pi, & \text{if } s = 0 \text{ and } m = k \neq 0) \\ \pi/2, & \text{if } k = m + s \text{ and } m \neq 0 \text{ and } s \neq 0 \\ \pi/2, & \text{if } s = m + k \text{ and } k \neq 0 \text{ and } m \neq 0 \\ \pi/2, & \text{if } m = s + k \text{ and } k \neq 0 \text{ and } s \neq 0 \\ 0, & \text{otherwise} \end{array} \right\}. \tag{13}$$

The maximum potential energy of the elastic, spiral, distributed springs which simulate the flexible rotational constraint at the radius R (see Figure 1) is given by

$$V_R = \frac{1}{2} \int_0^{2\pi} c(\theta) \left(\frac{\partial W}{\partial r}(R, \theta) \right)^2 R \, \mathrm{d}\theta. \tag{14}$$

Due to the assumed symmetry of the rotational constraint, the stiffness c (Newton) of the spiral, distributed spring can be expanded into the Fourier cosine series

$$c(\theta) = \sum_{k=1}^{\infty} c_k \cos(k\theta). \tag{15}$$

By using equations (10) and (15), the maximum potential energy V_R can be expressed as

$$V_R = \frac{1}{2} R \sum_{m=0}^{\infty} \sum_{s=0}^{\infty} \sum_{n=0}^{\infty} \sum_{i=0}^{\infty} \sum_{k=0}^{\infty} \psi_{msk} c_k a_{mn} a_{si} \frac{\partial W_{mn}}{\partial r}(R) \frac{\partial W_{si}}{\partial r}(R), \tag{16}$$

where

$$\frac{\partial W_{mn}}{\partial r}(R) = \begin{Bmatrix} 0, & \text{if } m = n = 0 \\ 2/a, & \text{if } m = 1 \text{ and } n = 0 \\ (\lambda_{mn}/a)[A_{mn} J'_m(\lambda_{mn} R/a) + C_{mn} I'_m(\lambda_{mn} R/a)], & \text{otherwise,} \end{Bmatrix}. \tag{17}$$

For antisymmetric modes, equation (1) can be written in the form

$$W(r, \theta) = \sum_{m=1}^{\infty} \sum_{n=0}^{\infty} W_{mn}(r) b_{mn} \sin(m\theta). \tag{18}$$

Upon inserting equations (9) and (18) in equation (8), the maximum potential energy V_T becomes

$$V_T = \frac{1}{2} R \sum_{m=1}^{\infty} \sum_{s=1}^{\infty} \sum_{n=0}^{\infty} \sum_{i=0}^{\infty} \sum_{k=0}^{\infty} \varphi_{msk} l_k b_{mn} b_{si} W_{mn}(R) W_{si}(R), \tag{19}$$

where

$$\varphi_{msk} = \int_0^{2\pi} \sin(m\theta) \sin(s\theta) \cos(k\theta)\, \mathrm{d}\theta = \begin{Bmatrix} \pi, & \text{if } k = 0 \text{ and } m = s \\ -\pi/2, & \text{if } k = m + s \\ \pi/2, & \text{if } s = m + k \text{ and } k \neq 0 \\ \pi/2, & \text{if } m = s + k \text{ and } k \neq 0 \\ 0, & \text{otherwise} \end{Bmatrix}. \tag{20}$$

Obviously in this case both the integers m and s start from 1. The maximum potential energy of the elastic, spiral, distributed spring for antisymmetric modes is

$$V_R = \frac{1}{2} R \sum_{m=1}^{\infty} \sum_{s=1}^{\infty} \sum_{n=0}^{\infty} \sum_{i=0}^{\infty} \sum_{k=0}^{\infty} \varphi_{msk} c_k b_{mn} b_{si} \frac{\partial W_{mn}}{\partial r}(R) \frac{\partial W_{si}}{\partial r}(R). \tag{21}$$

The Rayleigh quotient for the problem studied is given by

$$(V_P + V_T + V_R)/T^*. \tag{22}$$

Now only a finite number of modes is considered in the Rayleigh–Ritz expansion. The matrix $\mathbf{q}$ of the Fourier coefficients is introduced:

$$q_{mn} = \begin{Bmatrix} a_{mn}, & \text{for symmetric modes,} & m = 0, \ldots, N-1; n = 0, \ldots, \tilde{N} - 1 \\ b_{mn}, & \text{for antisymmetric modes,} & m = 1, \ldots, N; n = 0, \ldots, \tilde{N} - 1 \end{Bmatrix}. \tag{23}$$

In equation (23) N terms in the circumferential direction and $\tilde{N}$ in radial direction are used in the expansion of symmetric modes; N and $\tilde{N}$ will be chosen large enough to give the accuracy required.

The reference kinetic energy of the plate, equation (5), can be written in the concise notation

$$T_P^* = \tfrac{1}{2}\rho_P h a^2 \mathbf{q}^{\mathrm{T}} \mathbf{M}_P \mathbf{q}, \tag{24}$$

where M_P is a fourth order tensor, given by

$$(M_P)_{mnsi} = \begin{Bmatrix} 2\pi\delta_{ms}\delta_{ni}, & \text{if } m = 0 \\ \pi\delta_{ms}\delta_{ni}, & \text{if } m > 0 \end{Bmatrix}, \tag{25}$$

δ_{ms} is the Kronecker delta, as is δ_{ni}, and s and i have the same range of values as m and n, respectively. The maximum potential energy of the plate, equation (7), can be written as

$$V_P = \tfrac{1}{2}(D/a^2)\mathbf{q}^{\mathrm{T}} \mathbf{K}_P \mathbf{q}, \tag{26}$$

where the tensor $\mathbf{K}_P$ is given by

$$(K_P)_{mnsi} = \begin{Bmatrix} 2\pi\delta_{ms}\delta_{ni}\lambda_{mn}^4, & \text{if } m = 0 \\ \pi\delta_{ms}\delta_{ni}\lambda_{mn}^4, & \text{if } m > 0 \end{Bmatrix}. \tag{27}$$

The maximum potential energy stored by the elastic distributed spring, by using equations (12) and (19) can be written as

$$V_T = \tfrac{1}{2} R \mathbf{q}^{\mathrm{T}} \mathbf{K}_T \mathbf{q}, \tag{28}$$

where the tensor $\mathbf{K}_T$ is

$$(K_T)_{mnsi} = \sum_{k=0}^{\infty} \psi_{msk} l_k W_{mn}(R) W_{si}(R), \qquad \text{for symmetric modes,} \tag{29}$$

$$(K_T)_{mnsi} = \sum_{k=0}^{\infty} \varphi_{msk} l_k W_{mn}(R) W_{si}(R), \qquad \text{for antisymmetric modes.} \tag{30}$$

In equations (29) and (30) the sums on k are stopped, in numerical computations, at an integer value large enough to give the required accuracy. The maximum potential energy stored by the elastic, spiral, distributed spring, obtained from equations (16) and (21), is

$$V_R = (1/(2R))\mathbf{q}^{\mathrm{T}} \mathbf{K}_R \mathbf{q}, \tag{31}$$

where the tensor $\mathbf{K}_R$ is given by

$$(K_R)_{mnsi} = \sum_{k=0}^{\infty} \psi_{msk} c_k R^2 \frac{\partial W_{mn}}{\partial r}(R) \frac{\partial W_{si}}{\partial r}(R), \qquad \text{for symmetric modes,} \tag{32}$$

$$(K_R)_{mnsi} = \sum_{k=0}^{\infty} \varphi_{msk} c_k R^2 \frac{\partial W_{mn}}{\partial r}(R) \frac{\partial W_{si}}{\partial r}(R), \qquad \text{for antisymmetric modes.} \tag{33}$$

The problem is solved by minimizing the Rayleigh quotient, equation (22); this operation gives a Galerkin equation that reduces to an eigenvalue problem,

$$((D/a^2)\mathbf{K}_P + R\mathbf{K}_T + (1/R)\mathbf{K}_R)\mathbf{q} - \Omega^2 \rho_P h a^2 \mathbf{M}_P \mathbf{q} = 0, \tag{34}$$

Ω being the circular frequency (rad s^{-1}) of the plate. The corresponding non-dimensional equation gives the frequency parameter Λ of the plate:

$$(\mathbf{K}_P + (Ra^2/D)\mathbf{K}_T + (a^2/(RD))\mathbf{K}_R)\mathbf{q} - \Lambda^4\mathbf{M}_P\mathbf{q} = 0. \tag{35}$$

Obviously, when one is studying both the symmetric and the antisymmetric modes, two different Galerkin equations are obtained. It is interesting to note that the non-dimensional stiffness of the translational constraint is

$$l^*(\theta) = (Ra^2/D)l(\theta), \tag{36}$$

and the non-dimensional stiffness of the rotational constraint is

$$c^*(\theta) = (a^2/(RD))c(\theta). \tag{37}$$

2.1. IN-PLANE LOAD

The in-plane load gives an additional potential energy during the plate vibration that must be added to the numerator of the Rayleigh quotient, equation (22). The maximum potential energy connected with this phenomenon is [24]

$$V_L = \frac{1}{2}L\int_0^{2\pi}\int_0^R \{[\partial W/\partial r]^2 + [(1/r)(\partial W/\partial\theta)]^2\}r\,\mathrm{d}r\,\mathrm{d}\theta, \tag{38}$$

where L is the uniform in-plane tensile load (N/m) and the integration is extended to the radius R as a consequence of the compression due to the bolts being only in this area (see Figure 1). It is to be noted that a compressive load ($L < 0$) gives a negative energy that decreases the natural frequencies. Obviously, if the plate is subjected to another uniform in-plane load having a different origin, the integration must be extended to the outer radius a. Simple calculation gives

$$V_L = \frac{1}{2}L\sum_{m=0}^{\infty}\sum_{s=0}^{\infty}\sum_{n=0}^{\infty}\sum_{i=0}^{\infty}\delta_{ms}\sigma_m a_{mn}a_{si}\left\{\int_0^1 \frac{\mathrm{d}}{\mathrm{d}\rho}[W_{mn}(R\rho)]\frac{\mathrm{d}}{\mathrm{d}\rho}[W_{si}(R\rho)]\rho\,\mathrm{d}\rho\right.$$

$$\left. + m^2\int_0^1 \frac{W_{mn}(R\rho)W_{si}(R\rho)}{\rho}\,\mathrm{d}\rho\right\}, \tag{39}$$

where

$$\sigma_m = \begin{Bmatrix} 2\pi, & \text{if } m = 0 \\ \pi, & \text{if } m \geqslant 1 \end{Bmatrix}.$$

Equation (39) can be written in the concise form

$$V_L = \tfrac{1}{2}L\mathbf{q}^{\mathrm{T}}\mathrm{K}_L\mathbf{q}, \tag{40}$$

where the expression for $\mathbf{K}_L$ is easily obtained from equation (39). It also can be useful to introduce the following non-dimensional expression of the in-plane load:

$$L^* = (a^2/D)L. \tag{41}$$

3. VARIABLE SPRINGS DISTRIBUTED ON AN ANNULUS

By using the technique shown in section 2, it is possible to study a circular plate resting on an annular Winkler elastic foundation or a plate subjected to an elastic moment distributed on an annulus of its surface. Both the stiffness of the elastic foundation and the stiffness of the spiral, distributed springs are assumed to be variable according to the angular co-ordinate but to be uniform according to the radial co-ordinate. With this hypothesis, equations (9) and (15) are still correct, where the stiffness l now has the dimension (N m^{-3}) and c (N m^{-1}).

The lowest axisymmetric frequency of vibration of a circular plate partially embedded in a Winkler foundation was obtained by Laura *et al*. [26], who assumed the foundation stiffness to be constant. The free vibrations of circular plates with an elastic or rigid, interior, circular support having constant stiffness was studied by Azimi [27] using the receptance method. However, the problem studied in this section seems not to have been treated in the open literature.

The case of symmetric modes of a plate resting on an annular Winkler foundation is studied only because the other cases, antisymmetric modes and elastic moment distributed on an annulus, can be similarly investigated. The maximum potential energy stored by the elastic foundation is given by

$$V_F = \frac{1}{2}\int_0^{2\pi}\int_{a_1}^{a_2}\left(\sum_{k=0}^{\infty} l_k \cos(k\theta)\right)\left(\sum_{m=0}^{\infty}\sum_{n=0}^{\infty} W_{mn}(r)a_{mn}\cos(m\theta)\right)^2 r\,\mathrm{d}r\,\mathrm{d}\theta, \tag{42}$$

where a_1 is the inner radius of the annular foundation and a_2 is the outer radius of the foundation; obviously $a_1 < a_2 \leqslant a$. The result of the integration on θ is

$$V_F = a^2 \sum_{m=0}^{\infty}\sum_{s=0}^{\infty}\sum_{n=0}^{\infty}\sum_{i=0}^{\infty}\sum_{k=0}^{\infty} \psi_{msk} l_k a_{mn} a_{si} \sigma_{mnsi}, \tag{43}$$

where

$$\sigma_{mnsi} = \int_{e_1}^{e_2} [A_{mn}\mathrm{J}_m(\lambda_{mn}\rho) + C_{mn}\mathrm{I}_m(\lambda_{mn}\rho)][A_{si}\mathrm{J}_s(\lambda_{si}\rho) + C_{si}\mathrm{I}_s(\lambda_{si}\rho)]\rho\,\mathrm{d}\rho, \tag{44}$$

and $e_1 = a_1/a$ and $e_2 = a_2/a$. The integral on ρ in equation (44) involves products of two Bessel functions and is obtained by using equations (11.106), (31.101) and (33.101) in reference [28]. The final expression is not reported because it is quite tedious; however it gives no computational problems. The natural frequencies of the plate are still obtained by an eigenvalue problem, minimizing the Rayleigh quotient

$$(V_P + V_F)/T_P^*, \tag{45}$$

where V_P and T_P^* are given by equations (24) and (26).

4. NUMERICAL RESULTS AND DISCUSSION

All the results reported in this section are given in non-dimensional form, so that they may be applied to different geometries. In particular, the frequency parameter Λ is related to the circular frequency ω (rad/s) by

$$\Lambda = a\sqrt{\omega}/\sqrt[4]{D/(\rho_P h)}. \tag{46}$$

4.1. COMPARISON WITH PUBLISHED RESULTS

Numerical results were obtained for the problem studied in section 2 by truncating the infinite sums into 12 terms and using the *Mathematica* computer program [29]; therefore 144 modes were considered in the Rayleigh–Ritz expansion. In particular two different sets of modes were found. They are the symmetric and the antisymmetric modes with respect to the symmetry axis of the edge constraints.

In order to verify the accuracy of the proposed theory, the frequency parameters Λ of simply supported plates have been computed for $v = 0{\cdot}3$ by using the non-dimensional stiffnesses $l^* = 1800$ and $c^* = 0$. The first four frequency parameters are 2·22, 3·71, 5·02 and 5·41; the exact parameters are [7] 2·22152, 3·72803, 5·06096, 5·45161. The differences are less than 1%. Analogously, the frequency parameters of clamped plates have been computed by using the stiffnesses $l^* = 1800$ and $c^* = 80$. The first four frequency parameters are 3·25, 4·65, 5·70, 6·30; the exact parameters are [3] 3·1962, 4·6109, 5·9059, 6·3064.

The frequency parameters of symmetric modes of plates clamped along part of the edge and simply supported on the remainder were computed for $v = 0{\cdot}3$, the stiffness $l^* = 1800$ and expanding c^* into a Fourier series (first 12 terms). For plates clamped along 90°, the first three frequency parameters of symmetric modes are 2·53, 4·10, 5·17; only the parameter of the fundamental mode, computed for $v = 0{\cdot}25$, is available in the paper of Bartlett [14] and is 2·520 (upper bound) or 2·517 (lower bound); this is very close to the value obtained here. The results of Bartlett [14] are in good agreement with the results of Hirano and Okazaki [16]. Many more data are available in the paper of Narita and Leissa [12]; the first three frequency parameters of symmetric modes that they obtained for $v = 0{\cdot}3$ are 2·547, 4·131, 5·219.

For plates clamped along 180°, the first three frequency parameters are 2·76, 4·20, 5·41; only the value of the frequency parameter of the fundamental mode for $v = 0{\cdot}25$ is available in reference [14]: 2·740 (upper bound) or 2·735 (lower bound), that, again, is close to the value given here. The frequency parameter of the second mode (antisymmetric) for $v = 0{\cdot}25$ is available in Figure 4 of reference [16]; its numerical value is about 4·18. Also in this case many more data are available in the paper of Narita and Leissa [12]; the first three frequency parameters of symmetric modes that they obtained for $v = 0{\cdot}3$ are 2·770, 4·184, 5·536.

A comparison is also made with the results given in reference [11] for plates with no edge deflection and stiffness of the spiral, distributed spring $c^*(\theta) = c_0 + c_1 \cos(\theta)$; symmetric modes were computed. The first case considered is when $c_0 = 1$ and $c_1 = 0{\cdot}5$ for $v = 0{\cdot}3$. The frequency parameters are 2·46, 3·85, 5·11; only the first parameter is given in reference [11]: 2·46. The second case considered is when $c_0 = 5$ and $c_1 = 4{\cdot}5$ for $v = 0{\cdot}3$. The frequency parameters are 2·76, 4·08, 5·31; only the first parameter is given in reference [11]: 2·78.

An interesting boundary condition is that of a plate having half an edge clamped and half free; in the literature this problem has been studied by Narita and Leissa [13]. For this case the stiffnesses of l^* and c^* both must be expanded into a Fourier series; the stiffnesses for simulation of the clamped arc are 1250 for l^* and 80 for c^*. The first three computed frequency parameters of symmetric modes are ($v = 0{\cdot}3$) 1·50, 3·07, 3·60, 4·57; for antisymmetric modes they are 2·44, 4·35. Only terms having up to 11 waves were used in the Fourier expansion, so that more accurate results could be obtained by considering more terms. These results are in quite good agreement with those given in Figure 5 of the paper of Narita and Leissa [13]. Data obtained by a standard finite element code [30], by using 192 elements with eight nodes, are 1·56, 3·05, 3·80, 4·57 (symmetric modes) and 2·66, 4·45 (antisymmetric modes).

TABLE 1

Frequency parameters Λ of symmetric modes of circular plates having the spring stiffnesses $l^*(\theta) = 900 + 900\cos(N\theta)$ and $c^*(\theta) = 40 + 40\cos(N\theta)$, computed for $v = 0{\cdot}3$.

	Mode			
N	1st	2nd	3rd	4th
0	3·25	4·65	5·70	6·30
1	2·98	3·72	4·73	5·69
2	3·08	4·58	4·62	5·96
3	3·12	4·32	5·26	5·27
4	3·13	4·40	5·62	5·63
5	3·14	4·40	5·34	5·80
6	3·16	4·46	5·42	5·89
7	3·16	4·48	5·46	5·94

4.2. APPLICATION TO BOLTED OR RIVETED PLATES

Before applying the method to bolted plates, the frequency parameters of plates having the spring stiffnesses $l^*(\theta) = 900 + 900\cos(N\theta)$ and $c^*(\theta) = 40 + 40\cos(N\theta)$ at the edge are computed for different N values ($v = 0{\cdot}3$) for symmetric modes. The constant and the oscillating parts of the stiffnesses are chosen in order to have the plate almost clamped in N areas, and nearly free in between these areas. In fact, plates fixed with N bolts have boundary conditions that can be simulated by non-uniform flexible constraints; when expanding the stiffness of the constraints into Fourier series, the more important non-constant term is, obviously, the term having N waves. Therefore, the case studied gives a first idea of the problem. The computed frequency parameters are given in Table 1 for N varying from 1 to 7. The frequency parameter of the fundamental mode obviously increases with N, except for $N = 0$.

The study was next addressed to bolted or riveted plates. The constraints given by bolts (or rivets) can be assumed to be translational and rotational springs having high stiffness; these springs are located at the mean radius where bolts are placed and in a quite small area. Therefore the constraints can be expanded into Fourier series so that the Rayleigh–Ritz method can be applied. It must be observed that here the effect of damping due to friction at the bolted or riveted joint [31, 32] and all other nonlinear effects have been neglected.

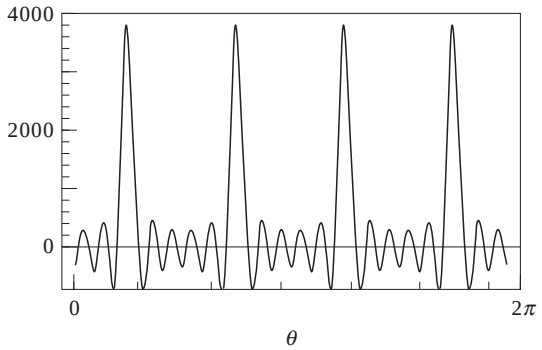

Figure 2. Fourier expansion of the stiffness $l^*(\theta)$ used for the bolted plate model (4 bolts).

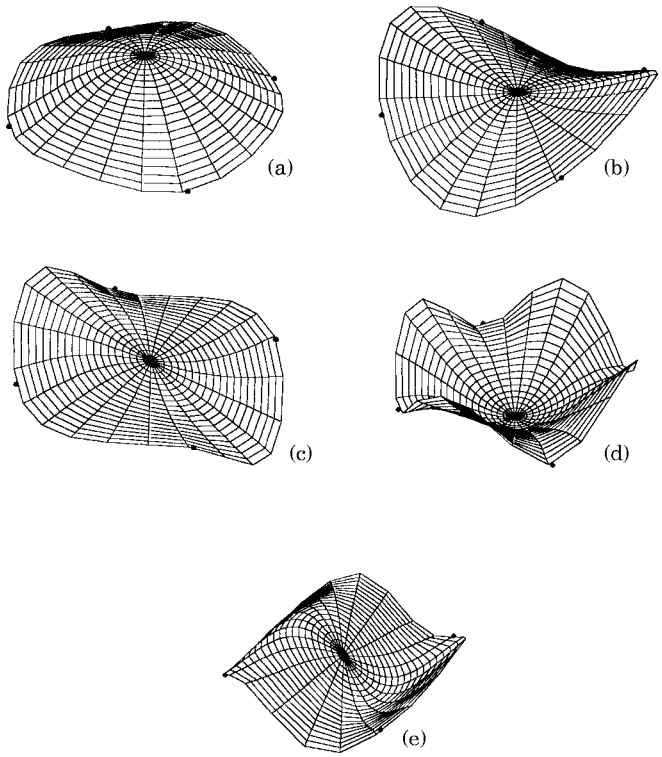

Figure 3. Symmetric mode shapes of the plate having four bolts; $R = a$. (a) $\Lambda = 2{\cdot}42$; (b) $\Lambda = 2{\cdot}72$; (c) $\Lambda = 2{\cdot}91$; (d) $\Lambda = 3{\cdot}71$; (e) $\Lambda = 4{\cdot}36$.

A circular plate bolted (riveted) with four bolts at the edge was simulated for $v = 0{\cdot}3$, by using the Fourier expansion of the stiffness l^* given in Figure 2 and having a maximum value of 3800. An analogous expansion was used to simulate c^*, where the maximum non-dimensional stiffness of the spiral spring is 80. The hypothetical stiffness function should be close to a step function, having a constant value on the angles corresponding to the bolt heads and zero otherwise; the non-zero constant segments can also be regarded as parabolic arcs. Obviously, as a consequence of the choice to limit the expansions of l^* and c^* to terms having up to 22 waves, only an approximation of the desired stiffness is possible. Hence, in Figure 2, a negative stiffness for some angles is shown, but it is not desired; a better approximation of the stiffness function can be obtained by using more terms. The first five symmetric mode shapes are given in Figure 3 and the first three antisymmetric mode shapes in Figure 4, where the frequency parameters are given in the explanations. In Table 2 the frequency parameters are satisfactorily compared to those obtained by using a standard finite element code [30]. In Figure 5 the corresponding mode shapes obtained by using the finite element method (FEM) are plotted; they are in good agreement with mode shapes given in Figures 3 and 4. One can observe that, according to this model, plates fixed by four bolts present mode shapes and natural frequencies which are quite different with respect to the modal characteristics of perfectly clamped plates.

It has previously been mentioned that bolts are located at a radius R internal to the edge. Therefore the study is addressed to a steel plate having the following characteristics: edge radius $a = 220$ mm, bolt radius $R = 197{\cdot}5$ mm, thickness $h = 5$ mm, Young's modulus $E = 206$ GPa, Poisson's ratio $v = 0{\cdot}3$; and mass density $\rho_P = 7800$ kg m^{-3}. The effect of the in-plane stress due to bolt pressure is neglected in this case. The natural frequencies

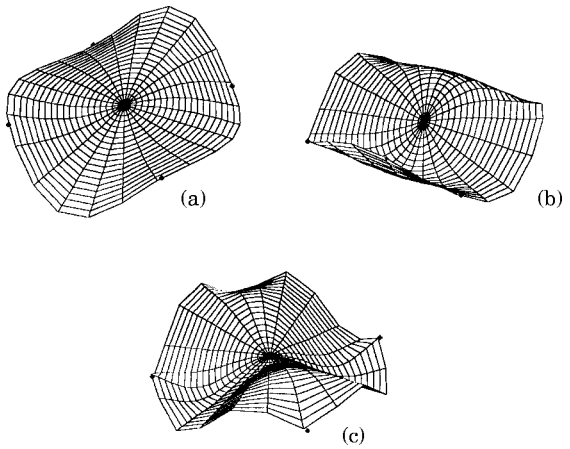

Figure 4. Antisymmetric mode shapes of the plate having four bolts; $R = a$. (a) $\Lambda = 2{\cdot}91$; (b) $\Lambda = 4{\cdot}36$; (c) $\Lambda = 4{\cdot}82$.

of the first four modes are given in Figure 6 as dashed line versus the number of equidistant bolts that fix the plate. It is to be noted that the second and third modes have the same frequency and shape but the first is symmetric and the second antisymmetric. In Figure 6 the results obtained by using the finite element method [30] are plotted as solid lines. In this finite element model the holes, that have a radius of 11 mm, have also been modelled; moreover the bolt constraints are imposed on all the holes, so that they are distributed over a larger area than in the previous model. Therefore the results obtained by using the FEM (solid line in Figure 6) are larger than those of the simplified model (dashed line). However both the models show that the bolt number largely affects the modal behaviour of a bolted plate. The first six modes of a plate fixed by eight bolts are given in Figure 7; the results have been obtained by using the FEM and also considering the holes. Significant differences from the modes of the plate fixed by four bolts can be detected.

5. CONCLUSIONS

The proposed method gives a simple formulation to compute both the frequency parameters, related to natural frequencies, and mode shapes of circular plates having elastic constraints varying according to the angular co-ordinate. It is particularly

TABLE 2

Frequency parameters Λ of modes of circular plates having four bolts; comparison of theoretical and FEM results and relative differences.

	Theory	FEM	Difference [%]
Symmetric	2·42	2·40	−0·8
	2·72	2·80	2·9
	2·91	2·94	1·0
	3·71	3·65	−1·6
	4·36	4·41	1·1
Antisymmetric	2·91	2·94	1·0
	4·36	4·41	1·1
	4·82	4·90	1·7

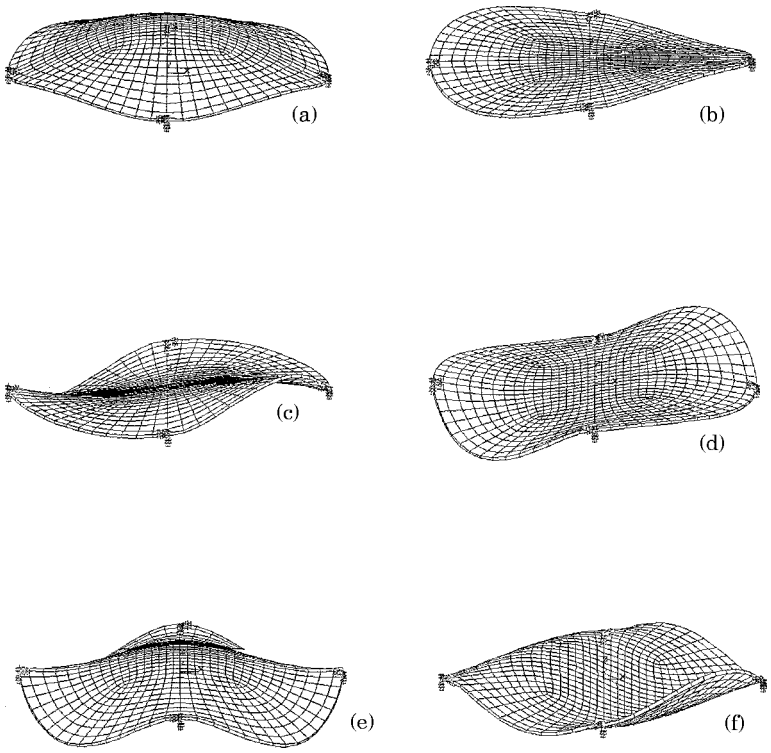

Figure 5. Mode shapes of the plate having four bolts obtained by the FEM; $R = a$. (a) $\Lambda = 2{\cdot}40$; (b) $\Lambda = 2{\cdot}80$; (c) $\Lambda = 2{\cdot}94$; (d) $\Lambda = 2{\cdot}94$; (e) $\Lambda = 3{\cdot}65$; (f) $\Lambda = 4{\cdot}41$.

suitable for realizing a computer program to solve quickly the eigenvalue problem. The accuracy of the numerical results depends on the number of modes retained in the series expansion of both mode shapes and stiffnesses of the constraints. Obviously, steep stiffness curves require more terms in the Fourier series expansion to obtain a good accuracy. However, even with quite a large number of modes in the expansion, the program can easily work on a personal computer. The method is also suitable to be used in conjunction with the artificial spring method to study quite complex structures where bolted or riveted circular plates are employed.

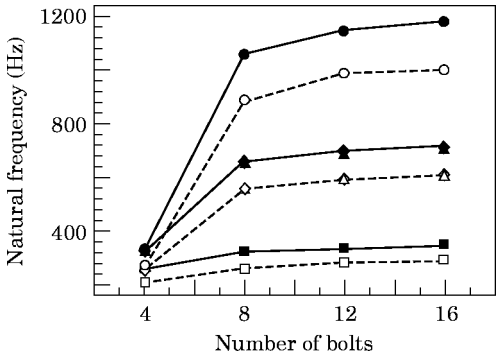

Figure 6. Natural frequencies (Hz) of the first four modes of the bolted plate; simplified model (dashed line) and FEM model (solid line). Mode numbers: —■—, - - -□- - -, 1st; —◆—, - - -◇- - -, 2nd; —▲—, - - -△- - -, 3rd; —●—, - - -○- - -, 4th.

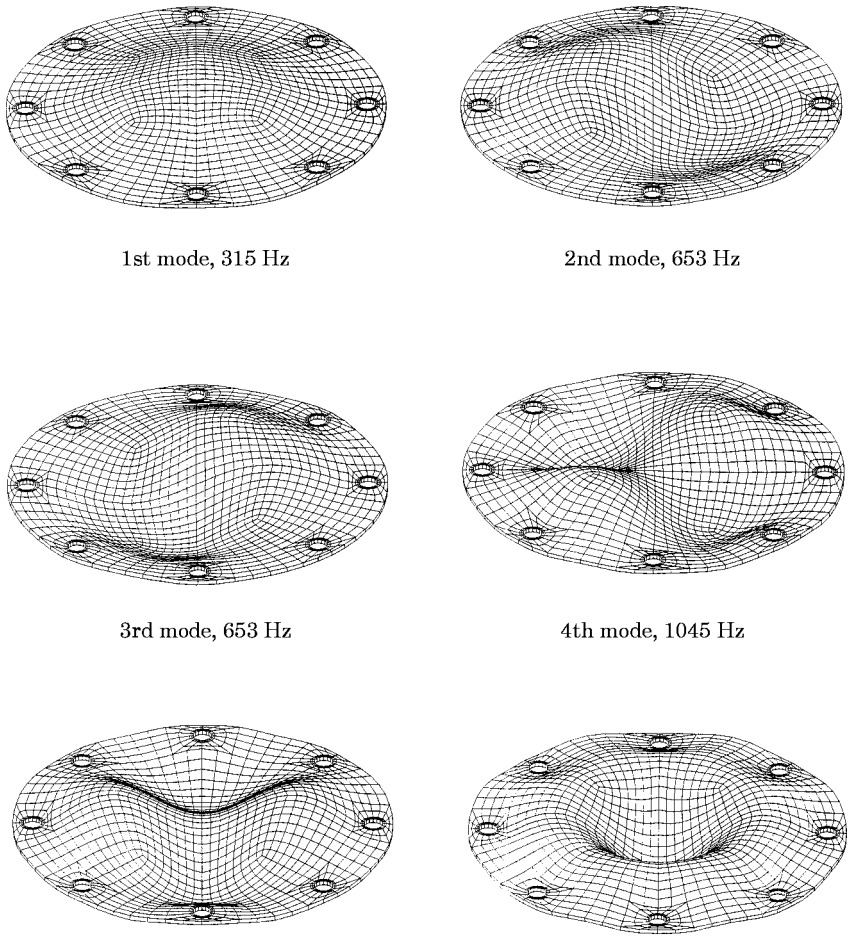

Figure 7. First six modes of the plate fixed by eight bolts as obtained by the FEM.

REFERENCES

1. S. D. Poisson 1829 *Memoires de l'Acadèmie Royale des Sciences de l'Institut de France*, ser. 2, **VIII**, 357. L'equilibre et le mouvement des corps elastiques.
2. G. Kirchhoff 1850 *Mathematical Journal* (*Crelle's Journal*) **40**, 51–58. Über das gleichgewicht und die bewegung einer elastischen scheibe.
3. A. W. Leissa 1969 *Vibration of Plates*, NASA SP-160. Washington, DC: Government Printing Office.
4. J. R. Airey 1911 *Proceedings of the Physical Society* (*London*) **23**, 225–232. The vibration of circular plates and their relation to Bessel functions. Also published in A. Kalnins and C. L. Dym 1976 *Vibration. Beam, Plates and Shells*, 60–67. Stroudsburg, USA: Dowden, Hutchinson & Ross.
5. R. C. Colwell and H. C. Hardy 1937 *Philosophical Magazine Series* 7, **24**, 1041–1055. The frequencies and nodal systems of circular plates.
6. K. Itao and S. H. Crandall 1979 *Transactions of the ASME, Journal of Applied Mechanics* **46**, 448–453. Natural modes and natural frequencies of uniform, circular free-edge plates.
7. M. Amabili, A. Pasqualini and G. Dalpiaz 1995 *Journal of Sound and Vibration* **188**, 685–699. Natural frequencies and modes of free-edge circular plates vibrating in vacuum or in contact with liquid.

8. A. W. Leissa and Y. Narita 1980 *Journal of Sound and Vibration* **70**, 221–229. Natural frequencies of simply supported circular plates.
9. S. Azimi 1988 *Journal of Sound and Vibration* **120**, 19–35. Free vibration of circular plates with elastic edge supports using the receptance method.
10. A. V. Bapat and S. Suryanarayan 1993 *Journal of Sound and Vibration* **163**, 463–478. A theoretical basis for the experimental realization of boundary conditions in the vibration analysis of plates.
11. A. W. Leissa, P. A. A. Laura and R. H. Gutierrez 1979 *Journal of the Acoustical Society of America* **66**, 180–184. Transverse vibrations of circular plates having non-uniform edge constraints.
12. Y. Narita and A. W. Leissa 1980 *Journal of Sound and Vibration* **70**, 103–116. Transverse vibration of simply supported circular plates having partial elastic constraints.
13. Y. Narita and A. W. Leissa 1981 *International Journal of Solids and Structures* **17**, 83–92. Flexural vibrations of free circular plates elastically constrained along parts of the edge.
14. C. C. Bartlett 1963 *Quarterly Journal of Mechanics and Applied Mathematics* **16**, 431–440. The vibration and buckling of a circular plate clamped on part of its boundary and simply supported on the remainder.
15. B. Noble 1965 *Developments in Mechanics* (*Proceedings of the* 9*th Midwest Conference*) **3**, 141–146. The vibration and buckling of a circular plate clamped on part of its boundary and simply supported on the remainder.
16. Y. Hirano and K. Okazaki 1976 *Bulletin of the Japan Society of Mechanical Engineers* **19**, 610–618. Vibration of a circular plate having partly clamped or partly simply supported boundary.
17. M. Amabili, G. Frosali and M. K. Kwak 1996 *Journal of Sound and Vibration* **191**, 825–846. Free vibration of annular plates coupled with fluids.
18. L. Meirovitch 1986 *Elements of Vibration Analysis* (2nd edition). New York: McGraw-Hill. See pp. 270–282.
19. J. Yuan and S. M. Dickinson 1992 *Journal of Sound and Vibration* **152**, 203–216. On the use of artificial springs in the study of the free vibrations of systems comprised of straight and curved beams.
20. J. Yuan and S. M. Dickinson 1992 *Journal of Sound and Vibration* **159**, 39–55. The flexural vibration of rectangular plate systems approached by using artificial springs in the Rayleigh–Ritz method.
21. M. Amabili, R. Pierandrei and G. Frosali 1996 *Proceedings of the Third European Conference on Structural Dynamics* **2**, 663–669, Rotterdam: Balkema. Comparative study of the modal behaviour of bolted and clamped plates.
22. P. A. A. Laura 1995 *Journal of Sound and Vibration* **180**, 815. Comments on "A theoretical basis for the experimental realization of boundary conditions in the vibration analysis of plates".
23. P. A. A. Laura, L. E. Luisoni and A. Arias 1976 *Journal of Sound and Vibration* **47**, 433–437. Antisymmetric modes of vibration of a circular plate elastically restrained against rotation and subjected to a hydrostatic state of in-plane stress.
24. D. J. Gunaratnam and A. P. Bhattacharya 1985 *Journal of Sound and Vibration* **102**, 431–439. Transverse vibration of circular plates having mixed elastic rotational edge restraints and subjected to in-plane forces.
25. N. S. Ferguson and R. G. White 1988 *Journal of Sound and Vibration* **121**, 497–509. The free vibration characteristics of a clamped-free disc under the action of a static in-plane load and constraint on the outer periphery.
26. P. A. A. Laura, R. H. Gutierrez, H. C. Sanzi and G. Elvira 1995 *Journal of Sound and Vibration* **185**, 915–919. The lowest axisymmetric frequency of vibration of a circular plate partially embedded in a Winkler foundation.
27. S. Azimi 1988 Journal of Sound and Vibration **120**, 37–52. Free vibration of circular plates with elastic or rigid interior support.
28. A. D. Wheelon 1968 *Tables of Summable Series and Integrals Involving Bessel Functions*. San Francisco: Holden-Day.
29. S. Wolfram 1991 *Mathematica*: *A System for Doing Mathematics by Computer* (2nd edition). Redwood, CA: Addison-Wesley.
30. *ANSYS User Manual* 1992, Revision 5. Houston, PA: Swanson.
31. Y. S. Shin, J. C. Iverson and K. S. Kim 1991 *Transactions of the ASME*, *Journal of Pressure Vessel Technology* **113**, 402–408. Experimental studies on damping characteristics of bolted joints for plates and shells.
32. L. Jézéquel 1983 *Transactions of the ASME*, *Journal of Vibration*, *Acoustics*, *Stress*, *and Reliability in Design* **105**, 497–504. Structural damping by slip in joints.